



POLİTEKNİK DERGİSİ

*JOURNAL of POLYTECHNIC*

ISSN: 1302-0900 (PRINT), ISSN: 2147-9429 (ONLINE)

URL: <http://dergipark.gov.tr/politeknik>



## Performance evaluation of bridges under scour by UAS based measurements

*Oyulma etkisindeki köprülerin İHS esaslı ölçümlerle performans değerlendirmesi*

*Yazar(lar) (Author(s)): Orkan ÖZCAN*

*ORCID: 0000-0002-7485-6157*

**Bu makaleye şu şekilde atıfta bulunabilirsiniz (To cite to this article):** Özcan O., "Performance evaluation of bridges under scour by UAS based measurements", *Politeknik Dergisi*, 22(2): 385-391, (2019).

**Erişim linki (To link to this article):** <http://dergipark.gov.tr/politeknik/archive>

**DOI:** 10.2339/politeknik.450288

# Performance Evaluation of Bridges Under Scour by UAS Based Measurements

*Araştırma Makalesi / Research Article*

**Orkan ÖZCAN**

Istanbul Technical University, Eurasia Institute of Earth Sciences, 34469, Maslak, Istanbul

(Received : 16.01.2018 ; Accepted : 22.06.2018)

## ABSTRACT

Flood and stream induced scour occurring in bridge piers located on rivers is one of the mostly observed failure reasons in bridges. Scour induced failure risk in bridges and determination of the alterations in bridge safety under seismic effects has the ultimate importance. Thus, for the determination of bridge safety under the scour effects, the scour amount under bridge piers should be designated realistically and updated with continuous monitoring. In this study, in order to measure the amount of scour in bridge piers unmanned aerial system (UAS) based measurement methods were implemented. UAS based measurement systems provide new and practical approach and bring high precision and reliable solutions considering recent measurement systems. For this purpose, the reinforced concrete (RC) bridge that is located on Antalya Boğaçayı River, Turkey and that failed in 2003 due to flood-induced scour was selected as the case study. The amount of scour occurred in bridge piers was determined realistically, and the behavior of bridge under scour effects was investigated. In the light of the attained scour measurements and expected scour after a probable flood event, the behavior of scour induced RC bridge was determined by pushover analyses under seismic loadings. In the analyses, the load and displacement capacity of bridge was observed to diminish significantly under expected scour. Regarding the case study, UAS based and continuously updated bridge performance evaluation system was developed that could be used for bridges located on the riverbed.

**Anahtar Kelimeler:** UAS, scour, bridge, performance.

## Oyulma Etkisindeki Köprülerin İHS Esaslı Ölçümlerle Performans Değerlendirmesi

### ÖZ

Nehir üzerinde bulunan köprü ayaklarında oluşan taşkın ve akış kaynaklı oyulma köprülerde çokça gözlemlenen göçme nedenlerinden biridir. Köprülerde oyulma kaynaklı göçme riski ve sismik etkiler altında köprü güvenliğinin değişimlerinin belirlenmesi büyük öneme sahiptir. Bu nedenle, oyulma etkileri altında köprü güvenliğinin belirlenmesi için köprü ayakları altındaki oyulma miktarının gerçekçi olarak belirlenmesi ve sürekli olarak izlenip güncellenmesi gereklidir. Bu çalışmada, köprü ayaklarındaki oyulma miktarının ölçülmesi için insansız hava sistemi (İHS) tabanlı ölçüm yöntemleri uygulanmıştır. İHS tabanlı ölçüm sistemleri yeni ve pratik bir yaklaşım sağlamakta ve günümüz ölçüm sistemleri düşünüldüğünde yüksek doğrulukta ve gerçekçi çözümler getirmektedir. Bu amaçla, Antalya Boğaçayı Nehri üzerinde bulunan ve 2003 yılında taşkın kaynaklı oyulma nedeniyle göçmüş betonarme (BA) köprü durum çalışması olarak seçilmiştir. Köprü ayaklarında oluşan oyulma miktarı gerçekçi olarak belirlenmiş ve oyulma etkileri altında köprü davranışı incelenmiştir. Elde edilen oyulma ölçümleri ve olası taşkın sonucu beklenen oyulma ışığında, oyulma etkisi altındaki BA köprüünün davranışı sismik yüklemeler altında itme analizi ile belirlenmiştir. Analizlerde köprüünün yük ve yer değiştirme kapasitesinin beklenen oyulma altında belirgin olarak azaldığı gözlemlenmiştir. Durum çalışmasına ilişkin olarak, İHS tabanlı ve sürekli olarak güncellenen ve nehir yatağında bulunan köprüler için kullanılacak performans belirleme sistemi geliştirilmiştir.

**Anahtar Kelimeler:** İHS, oyulma, köprü, performans.

### 1. INTRODUCTION

The vulnerability and consequent risk of RC bridges located on riverbeds under natural hazards such as stream/flood induced scour and earthquake has the ultimate importance for design and assessment. While scouring in bridge substructures constitutes a substantial part of major failure mechanisms observed in bridges [1, 2], pier scour measurements should be continuously implemented and updated accordingly. Thus, in

performance evaluation of RC bridges, scour depth at piers and piles should be accurately measured in order for more reliable bridge evaluation. There has been put much effort in developing methods for field scour measurements to assess current bridge condition or to forecast future behavior. In this respect, sonar [3] and ground-penetrating radar (GPR) [4] based measurement methods were implemented. In addition, pier scour depth was acquired by monitoring the change in bridge vibration characteristics by mounting accelerometers on bridges [5]. Radio frequency identification (RFID) method was utilized to measure instantaneous scour

\*Sorumlu yazar (Corresponding Author)  
e-posta : ozcanorkan@itu.edu.tr

depth while locating sensors on bridge piers [6]. However, the aforementioned methods have drawbacks of either being impractical or having high installation costs as compared to direct field measurement methods. Unmanned aerial vehicles (UAVs) have been utilized for flood analysis [7, 8], to the contrary, no UAS based scour measurement techniques were encountered in previous studies.

In the previous studies conducted in scour monitoring research field, the need of special equipment such as sonar, GPR, accelerometer, RFID highly increased the measurement costs and thus impeded the continuous tracking of scouring at bridge piers. Thus, by using the UAS measurement methods, the implementation time and measurement costs were monitored to decrease substantially.

In former studies, three-dimensional (3D) dense point-cloud generation workflows were investigated by UAV derived aerial imagery and accuracy analyses were substantiated via independent digital surface models (DSMs) as well as dataset of verification points. Herein, the accuracies obtained by Structure from Motion (SfM) technique were demonstrated to be comparable to traditional high-resolution topographical survey methods. The accuracy of the implemented SfM technique via UAV derived images was investigated for the regions having different geomorphic properties [9, 10]. In vast terrains, regarding UAV imagery based on SfM point clouds, the results of the studies were directed towards redetermination of changing topography and applications were compared with the outputs of high-resolution data acquisition techniques (Table 1). Terrestrial laser scanning (TLS) was used to map 80 m height cliffs and the accuracy of the DSM was determined to be lower than 0.5 m for 86% of the area [11]. The erosion rate was investigated using the DSM time series while comparing SfM and TLS data and the root mean square (RMS) error was 0.07 [12] and maximum deviation was determined as 0.1 m in a similar study [13]. In riverbed system, SfM and aerial LIDAR data were compared and the average variation between the regenerated topography by two different methods was indicated as 0.6 m [14].

Cirque glaciers were investigated by evaluating UAV-SfM data with the measured points with tachometric survey and vertical RMS error was 0.52 m while the lands with low plant cover the error was 0.2 m [15]. Direct referencing the point clouds that were derived by the UAV on which global navigation satellite system (GNSS) sensor was located and referencing by ground control points (GCPs) were compared and the horizontal accuracy of GCP derived orthomosaic images were observed to enhance 5 to 10 times [16]. In addition, the collocation of UAV and SfM algorithm was proposed to designate sub-decimeter variations [17]. In addition to nadir photos, the DSM generated by adding the oblique images in SfM algorithm was compared with GCPs and accuracies were obtained in a range between 0.001-0.083 m, 0.04-0.06 m in horizontal and vertical directions,

respectively. The utilization of UAV and SfM derived orthomosaic images and DSMs were demonstrated in order to determine landslide induced relative surface displacements [18].

**Table 1.** UAV-SfM based researches and accuracies.

| Ref. | Data set          | Method                                 | Accuracy   | Geo. Ref.   |
|------|-------------------|--|--|-------------|
| [11] | UAV-TLS           | SfM-DSM difference                     | 86% of area, 0.3-0.5 m                                   | Manual      |
| [12] | UAV-TLS           | SfM-DSM difference                     | Vertical RMSE 0.07 m                                     | Manual      |
| [13] | UAV-TLS           | SfM-DSM difference                     | Max. standard dev. 0.1 m                                 | N/A         |
| [14] | UAV-ALS           | SfM-DSM difference                     | Average difference 0.6 m                                 | Manual      |
| [15] | UAV-Total Station | SfM-Verification Points                | Vertical RMSE 0.52 m                                     | Manual      |
| [16] | UAV-DGPS          | SfM-Verification Points                | Average absolute horizontal accuracy 0.10-0.13 m         | GCP         |
| [16] | UAV-Internal GPS  | SfM-Verification Points                | Average absolute horizontal accuracy 0.66-1.25 m         | Direct      |
| [17] | UAV-SfM           | SfM-Verification Points                | Horizontal RMSE 0.001-0.083 m, Vertical RMSE 0.04-0.06 m | GCP         |
| [19] | RTK-GPS           | SfM-DSM Difference-Verification Points | Average absolute difference 0.074 m                      | GCP         |
| [20] | UAV-SfM-LIDAR     | SfM-DSM Difference-Verification Points | Average absolute difference 0.04 m                       | Direct, GCP |
| [21] | UAV-TLS           | SfM-DSM Difference-Verification Points | Standard deviation 0.61-1.26 cm                          | GCP         |

The accuracy of 3D topographical modeling was shown to be dependent on the used software to run SfM algorithm by comparing the reference real time kinematic (RTK) and GNSS data [19-21]. Along with the aforementioned studies, for modeling of river bathymetry by UAVs, the bathymetric data acquired from high-resolution images at shallow water were verified with real data and high correlation was obtained [22]. Since the complicated behavior of the bridges under scouring entailed that to be one of the most active research topics in engineering, most of the conducted research covered model generation studies related to local scour behavior. The recent researches revealed scour to be one of the main reasons responsible for the bridge failure. Within

this context, the behavior of scour influenced laterally loaded pile groups was determined by analytical studies and the lateral capacity of the pile groups were observed to increase and the maximum internal forces decrease with increasing scour depth. In addition, river bridges exposed to scour were modeled and the effect of bridge substructure capacity on bridge performance was assessed [23].

## 2. MATERIAL and METHOD

In order to acquire the lateral performance of bridges, many methods were implemented by means of basic beam and finite element modeling. Since most of the conducted research in this field focused on the column performances, the researches on scouring and earthquake performance of bridges with pile foundations gains currency in multi-disciplinary research fields. In this regard, although the use of UAS technology is increasing in many research fields, there were no research conducted in order to investigate the RC bridge substructures with UAS data. Herein, the scour depths at bridge piles was determined by UAS based measurements at shallow and clear water. The implemented UAS based scour monitoring method provided input data for performance assessment analyses of bridges while ensuring a fast, easy to implement and economic measurement method as compared to previous methods based on sonar, GPR, RFID and accelerometer sensors.

In this study, the DSM of the riverbed including the bridge and the scour depths at bridge substructures (piles and piers) were measured in 3Ds by UAS. In order to determine the variations in river topography, SfM technique was implemented while using the difference between DSMs that were obtained at different time intervals. The model of 3D structures such as bridges was generated using motion data integrated 2D image clusters in SfM technique. Herein, model geometry, position and orientation data were solved simultaneously and automatically. In order to find the relation between the images, the sensed features such as corners and sides was monitored from one image to another. Then, the feature trajectories were used for estimating the 3D location of the object and camera movement. Thus, the orthophotos and DSMs that were obtained by data acquisition methods were generated based on SfM algorithm.

The four fundamental steps in SfM can be specified as: (a) Bundle adjustment in which common nodes on overlapping photos were determined and matched in order to calculate camera parameters for the correction of each photo and camera calibration parameters. (b) For generation of dense point cloud, the node locations were calculated by specified camera locations and photos by using the stereo photogrammetric equations. (c) 3D polygon mesh model was generated while representing surface depending on the dense point cloud. (d) Regenerated mesh model was used for orthophoto generation in which DSM was calculated by interpolating

irregular polygon mesh model onto regular grids (Figure 1).

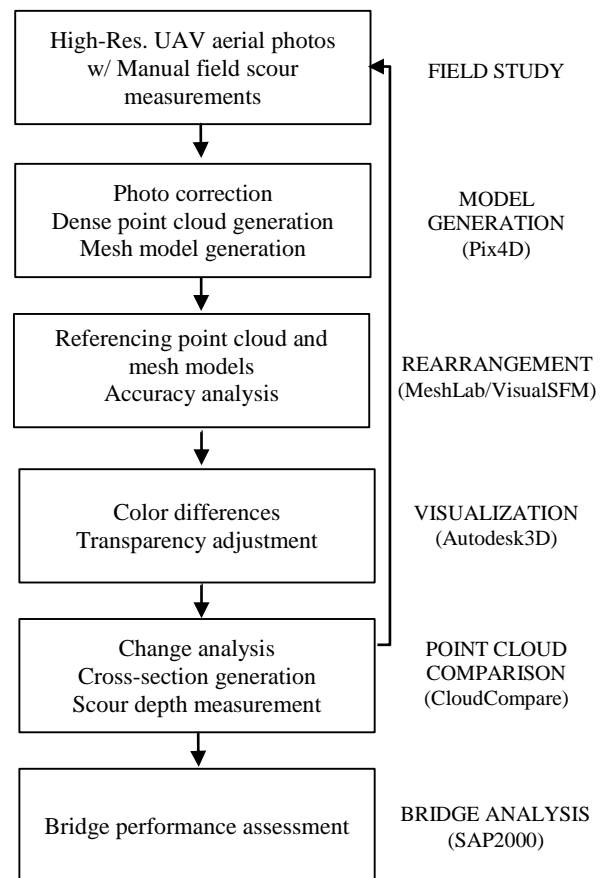


Figure 1. Workflow of UAS.

Therefore, the DSMs and orthophotos that were acquired using UAS based field measurements were calculated using SfM algorithm. Considering the UAS configuration, probable large-scale deformations in generated DSMs were reduced by manual field measurements. The frontal and lateral overlapping ratios in direction of motion and in between flight routes for aerial photos taken at surfaces covered with sand or having shallow water with low visual contents were determined as at least 85 and 70%, respectively. High-resolution aerial photos over the riverbed were obtained from nadir view at 70 m flight height. Moreover, for scour depth analysis, the scour depth under bridge piers was derived by oblique view (adjusting the camera angle to 45°) during the flight and the 3D model of the surface along bridge piers was obtained by manual designation of the flight heights such that photos could be taken at each view of the bridge with varying camera angles. The ground sampling distance (GSD) was used as 1 to 2 cm/pixel for the flights performed at these altitudes. In addition, the flight speed was reduced in order to provide more proper overlapping. Hereby, the acquired high-resolution orthophotos and dense point clouds were used to measure scour depths at bridge piers. The concordant

studies demonstrated that the measurements taken at shallow and clear water had a high correlation with the manual measurements [22].

As shown in the workflow (Figure 1), the images obtained from UAVs during the field study were processed, 3D dense point clouds were generated and high-resolution DSMs were constituted in model generation part. The rearrangement part constituted reorganization and referencing of the generated 3D dense point cloud and the mesh models. Herein, the subsisting artifacts were removed and the model was rearranged by open source software VisualSfM using SfM algorithm. In 3D data processing, volumetric calculations from closed mesh models or triangulated irregular network (TIN) for eroded geomorphology, which generally comprised open and hollow landforms, the generated mesh structure was transformed into closed mesh model by placing a plane on the mesh model [21]. The mesh models acquired at different dates were referenced to each other by applying 3D rotation matrix using open source software (MeshLab and VisualSfM). In order to minimize the resolution differences, the scale of SfM generated point clouds were reduced and resampled according to the data with the lowest resolution. After the visualization section in which color difference and transparency adjustments were considered, variation analysis was conducted by point cloud comparison using the CloudCompare software. Hereby, the diachronic generation of high-resolution DSMs for the same regions provided monitoring and mapping of erosion and accumulation, calculating the volumetric variation in time and designating sediment supply. The erosion and accumulation were acquired by calculating the difference between the DSMs that were obtained from the last and first measurements. The seasonal trend of morphological variation was monitored by the variation analysis in which the difference between DSMs obtained at different time intervals was taken into account. This difference in time intervals was shown as a backward arrow in the workflow. Afterwards, bridge performance assessment was conducted for measured scour depths at each bridge pier and pile. Herein, the 3D structural finite element model (FEM) of the bridge was generated by using design drawings and local soil conditions. The bridge performance under UAS-measured scour was determined by means of lateral pushover analysis.

### 2.1. Case Study – Antalya Boğaçayı Bridge

The UAS based assessment method was applied to Boğaçayı Bridge located on Boğaçayı River in Antalya Province, Turkey (Figure 2). The bridge spans were 20.3 m long between 14 piers including two abutments at the ends. Each pier had three 2.8 m tall columns with 1×2 m cross-section that were aligned such that the weak axis of the columns was parallel to the longitudinal axis of the bridge. The abutments had cross-section dimensions of 1.2×14 m having the same height as the piers. The piers and abutments were connected to a strong pile cap (3×15×1.5 m) that consisted 12 m long and 1 m diameter piles.

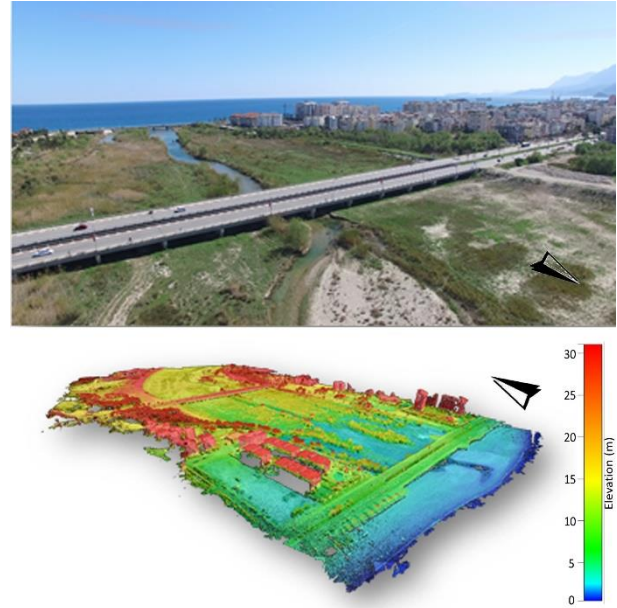


Figure 2. The Study Region – Boğaçayı Bridge.

Besides, there were pier caps and elastomeric bearings at the top of each pier cap that supported eight girders spanning through the bridge. As the current bridge condition, which was directly taken from the project drawings, the sand layer was present at the top of each pile cap and a limestone layer was found down to 5.5 m measured from the top of pile cap. Remaining layers beneath that level consisted sand layers. UAS based measurement method was directly applied to the bridge in a seasonal manner and the bridge cross-section data in longitudinal and transverse directions were used to monitor scour depths. Thus, scour depth and related parameters such as the bridge substructure condition related to the scour amount and consequent bridge performance was directly assessed.

### 3. RESULTS

In the first part of the study, a dense point cloud of the study region was acquired by using UAS derived high-resolution aerial photos as shown in Figure 2. Herein, it can be implied that during the summer season when the surface runoff was the minimum, clearest scour measurements were obtained. Since there was almost no stream in the river, the misleading results due to the refraction of light were minimized. The reliability of the acquired results was controlled via comparing with manual field measurements during which the field observations matched well with the UAV measurements (Figure 3). During the first measurements that were taken after the current condition in fall and spring seasons (Oct. and May), approximately 1.0 m of scouring relative to the current condition was monitored at the bottom of seventh and the eighth piers. The following seasonal measurements taken in summer season (July) denoted a scour depth of 2.2 m and the following measurements in



fall season indicated close scour depths (Figure 4). As can be observed from the transverse cross-sections were taken along all piers, the scour was concentrated on the seventh and the eighth piers through which the river was generally streaming.

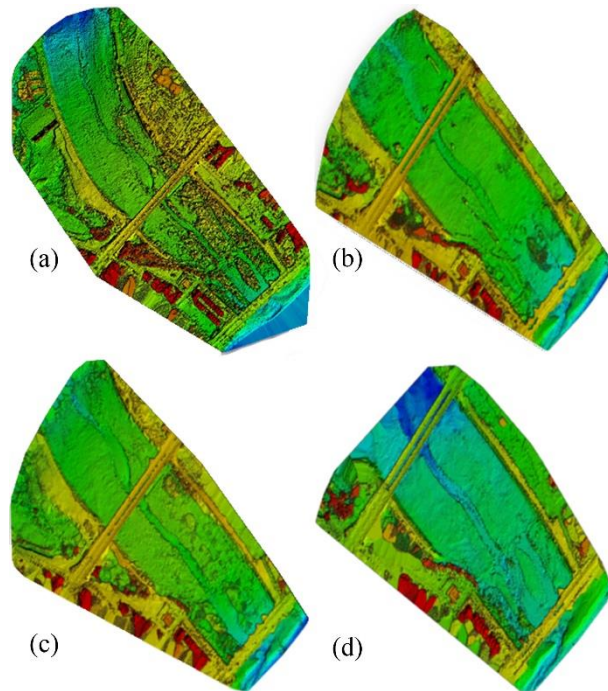


**Figure 3.** Seasonal changes of the study region in (a) fall, (b) winter, (c) spring and (d) summer.

At the other pier locations where the riverbed had almost no water flow during the year, the amount of scour was monitored to be approximately constant. Herein, for modeling of the bridge, SAP2000 program inputs were automatically generated with regard to the measured scour depths that were considered as an input for the following performance analysis.

obtained from the performance analyses implied that the increase in scour depths had almost no significant influence on the bridge lateral and longitudinal performance until the scouring reached the top of pile caps. Thus, the performance analysis was repeated for additional scour depths of 4.95 and 7.45 m below current soil altitude. As the scour reached the limestone layers, the bridge performance in lateral direction was observed to diminish drastically; however, no significant influence was recorded in the longitudinal direction (Figures 5a and 5b). This phenomenon was attributed to change of failure type in direction. Herein, there were no hinges formed in the piles in longitudinal direction whereas in the transverse direction the failure formed by hinging at the piles that were exposed to scour.

**4. DISCUSSION AND CONCLUSION**

The UAS based bridge tracking system was generated and implemented at a bridge located at Boğaçayı River in Antalya Province, Turkey as a case study. The proposed method was observed to measure the scour depths realistically and very close to the manual measurements obtained in the field study. The transverse cross-sections along bridge piers were tracked seasonally by UAV flights. The measured scour depths were used automatically in the structural model generation and consequently in seasonal performance assessment of the bridge.

The SAP2000 input files were created in .s2k format by an algorithm that was generated in MatLab programming language. Herein, by using the scour measurements by means of the UAS, the output file was generated that included the scoured soil levels at pier locations (Figure 1). The locations of the pier and piles are fixed. Therefore, only the properties of the nonlinear link elements, which were assigned to the piles at several heights, were changed. Subsequently, the structural

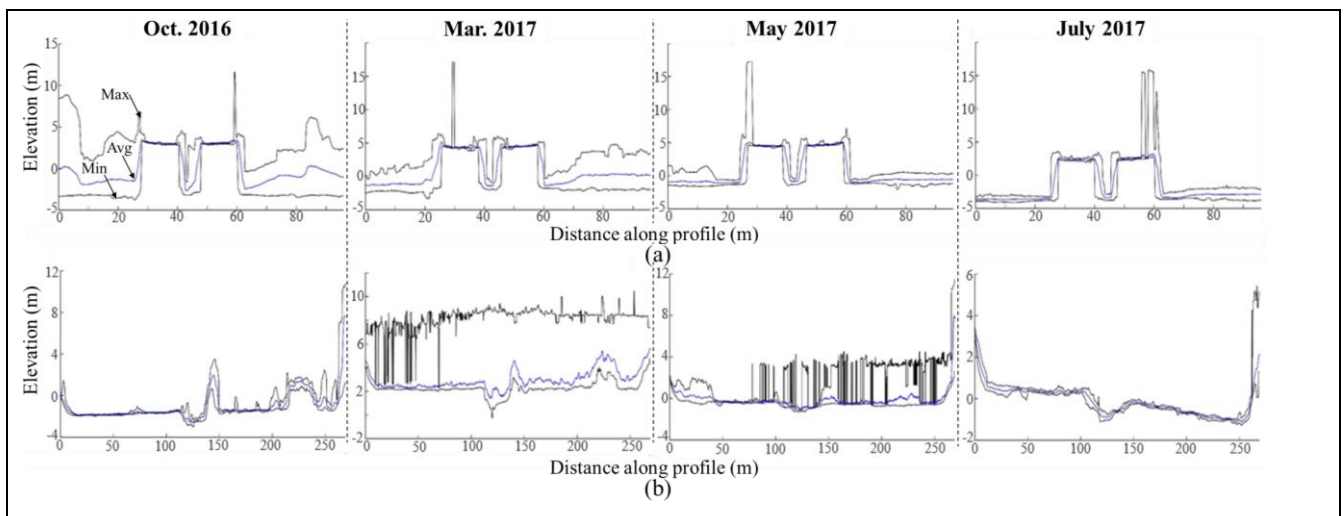


**Figure 4.** Seasonal changes in (a) transverse and (b) longitudinal cross-sections.

Thus, considering the results of each measurement, a new performance analysis was conducted. The results

system was reconstituted by SAP2000 regarding the different scoured soil depths. For the performance

analysis, the pushover curves were acquired by using SAP2000 nonlinear static analysis option. Since the primary goal of this research was to assess the functionality of the UAS based scour monitoring system, earthquake or flood based evaluation methods were not implemented.

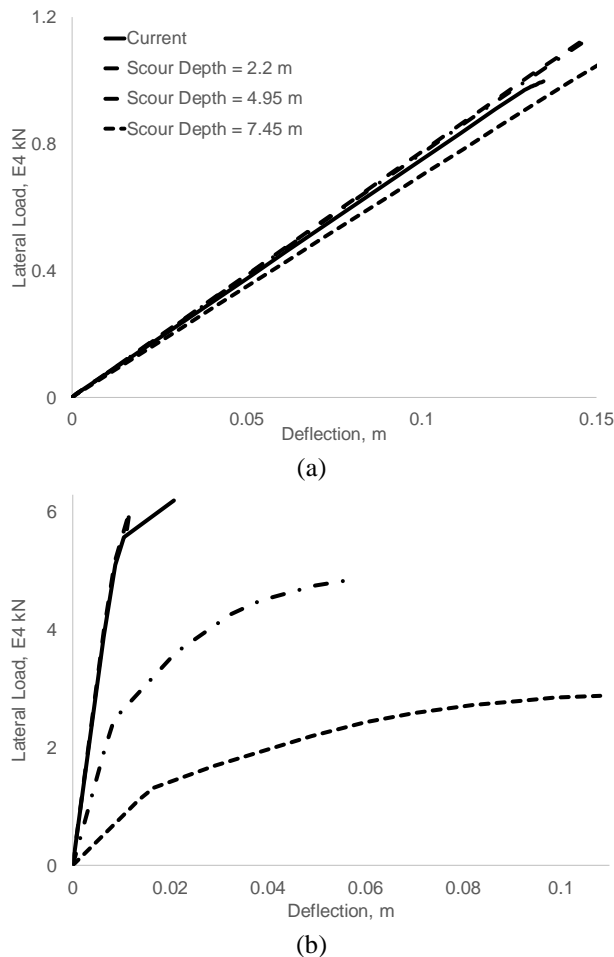


**Figure 5.** Bridge lateral capacity curves in (a) longitudinal and (b) transverse direction.

The amount of scour was monitored more successfully in the summer season when the surface runoff was the minimum and the misleading results due to light refraction were reduced. The maximum amount of scour was observed at the middle piers through which the river was streaming. Herein, for the bridge under investigation, the lateral performance was observed to diminish with the increase in scour depths beyond the pile cap. However, there was almost no influence on the performance in the longitudinal direction. Since the failure initiated with plastic hinging in the piers instead of the piles in the longitudinal direction, there were no performance change in longitudinal direction. However, since the bridge failed with plastic hinging at the pile critical locations, the scour depth was observed to have a significant effect on bridge transverse capacity. Thus, it can be inferred that the UAS based bridge tracking

system can be successfully used for bridges constructed at deep valleys and at the rivers having several soil layers.

## ACKNOWLEDGEMENT

The author would like to thank Assoc. Prof. Dr. Okan ÖZCAN for his valuable advise on modeling issues and constructive recommendations on various technical issues examined in this study.

## REFERENCES

- [1] Prendergast, L.J., Gavin, K., "A Review or Bridge Scour Monitoring Techniques" *Journal of Rock Mechanics and Geotechnical Eng.*, 6: 138-149, (2014).
- [2] Fisher, M., Chowdury, M.N., Khan, A.A., Atamtürktür, S., "An Evaluation of Scour Measurement Devices", *Flow Measurement and Instrumentation*, 33: 55-67, (2013).
- [3] DeFalco, F., Mele, R., "The Monitoring of Bridges for Scour by Sonar and Sedimetri", *NDT&E International*, 35: 55-67, (2002).
- [4] Burrell, J., Gurrola, H., Mickus, K., "Frequency Domain Electromagnetic and Ground Penetrating Radar Investigation of Ephemeral Streams: Case Study near the Southern High Plains, Texas", *Environmental Geology*, 55: 1169-1179, (2008).
- [5] Prendergast, L.J., Hester, D., Gavin, K., O'Sullivan, J.J., "An Investigation of the Changes in Natural Frequency of a Pile Affected by Scour", *Journal of Sound and Vibration*, 332: 6685-6702, (2013).
- [6] İbrahimy, M.I., Motakabber, S.M.A., "Bridge Scour Monitoring by Coupling Factor between Reader and Tag Antennas of RFID System", *International J. of Geomate*, 8(16): 1328-1332, (2015).
- [7] Tamminga, A.D., Eaton, B.C., Hugenholtz, C.H., "UAS Based Remote Sensing of Fluvial Change Following an Extreme Flood Event", *Earth Surface of Processes & Landforms*, 40: 1464-1476, (2015).
- [8] Jaud, M., "Potential for UAVs for Monitoring Mudflat Morphodynamics: Application to Seine Estuary, France", *ISPRS International Journal of Geo-Information*, 5: 50-55, (2016).
- [9] Javernick, L., Brasington, J., Caruso, B., "Modeling the Topography of Shallow Braided Rivers using Structure - from - Motion Photogrammetry", *Geomorphology*, 213: 166-182, (2014).
- [10] Verhoeven, G., Doneus, M., Briese, C., Vermeulen, F., "Mapping by Matching: A Computer Vision-Based Approach to Fast and Accurate Georeferencing of Archeological Aerial Photographs", *J. of Archeological Sci.*, 39: 2060-2070, (2012).
- [11] Westoby, M.J., Brasington, J., Glasser, N.F., Hambrey, M.J., Reynolds, J.M., "Structure-from-Motion Photogrammetry: A Low Cost Effective Tool for Geoscience Applications", *Geomorphology*, 179: 300-314, (2012).
- [12] James, R.M., Robson, S., "Straightforward Reconstruction of 3D Surfaces and Topography with a Camera: Accuracy and Geoscience Application", *J. of Geophysical Research*, 117: (2012).

- [13] Obanawa, H., Hayakawa, Y., Saito, H., Gomez, C., "Comparisons of DSMs Derived from UAV-SfM Method and Terrestrial Laser Scanning", *Journal of the Japan Society of Photogrammetry and Remote Sensing*, 53: 67-74, (2014).
- [14] Fonstad, M.A., Dietrich, J.T., Courville, B.C. Jensen, J.L., Carbonneau, P.E., "Topographic Structure from Motion: A New Development in Photogrammetric Measurement", *Earth Surface Processes and Landforms*, 38: 421-430, (2013).
- [15] Tonkin, T.N., Midgley, N.G., Graham, D.J., Labadz, J.C., "The Potential of Small Unmanned Aircraft Systems and Structure-from-Motion for Topographic Surveys: A Test of Emerging Integrated Approaches for Cwm Idwal, North Wales", *Geomorphology*, 225: 35-43, (2014).
- [16] Turner, D., Lucieer, A., Watson, C., "An Automated Technique for Generating Georectified Mosaics from Ultrahigh Resolution Unmanned Aerial Vehicle (UAV) Imagery based on Structure from Motion (SfM) Point Clouds", *Remote Sensing*, 4: 1392-1410, (2012).
- [17] Harwin, S., Lucieer, A., "Assessing the Accuracy of Georeferenced Point Clouds Reduced via Multi-view Stereopsis from Unmanned Aerial Vehicle Imagery", *Remote Sensing*, 4: 1573-1599, (2012).
- [18] Lucieer, A., DeJong, S.M., Turner, D., "Mapping Landslide Displacements using Structure from Motion (SfM) and Image Correlation of Multi-Temporal UAV Photography", *Progress in Physical Geography*, 38: 97-116, (2014).
- [19] Quedraogo, M.M., Degre, A., Debouche, C., Lisein, J., "An Evaluation of Unmanned Aerial System based Photogrammetry and Terrestrial Laser Scanning to Generate DEMs of Agricultural Watersheds" *Geomorphology*, 214: 339-355, (2014).
- [20] Clapuyt, F., "Reproducibility of UAV-based Earth Topography Reconstructions based on Structure from Motion Algorithms", *Geomorphology*, 260: 4-15, (2016).
- [21] Kaiser, A., Neugirg, F., Rock, G., Müller, C., Haas, F., Ries, J., Schmidt, J., "Small Scale Surface Reconstruction and Volume Calculation of Soil Erosion in Complex Moroccan Gully Morphology using SfM", *Remote Sensing*, 6: 7050-7080, (2014).
- [22] Flener, C., "Calibrating Deep Water Radiance in Shallow Water: Adapting Optical Bathymetry Modeling to Shallow River Environments", *Boreal Environmental Research*, 18: 488-502, (2013).
- [23] Lin, C., Bennett, C., Han, J., Parsons, R.L., "Scour Effects on the Response of Laterally Loaded Piles considering Stress History of Sand", *Computational Geotechnics*, 37: 1008-1014, (2010).